Author(s): Manzato, Claudio & Foster, Adam S. & Alava, Mikko J. & Laurson, Lasse

Title: Friction control with nematic lubricants via external fields

Year: 2015

Version: Final published version

Please cite the original version:

Manzato, Claudio & Foster, Adam S. & Alava, Mikko J. & Laurson, Lasse. 2015. Friction control with nematic lubricants via external fields. Physical Review E. Volume 91, Issue 1. 012504/1-6. ISSN 1539-3755 (printed). DOI: 10.1103/physreve.91.012504.

Friction control with nematic lubricants via external fields

Claudio Manzato, Adam S. Foster, Mikko J. Alava, and Lasse Laurson
COMP Centre of Excellence, Department of Applied Physics, Aalto University, P.O. Box 11100, Aalto 00076, Finland
(Received 27 May 2014; revised manuscript received 22 October 2014; published 12 January 2015)

We study the connection between sliding friction and the phase behavior of a simple rigid bead-necklace model of a liquid crystal (LC) lubricant layer confined between two parallel plates. The dynamics is dependent on competing LC ordering mechanisms, including the direction of sliding, and an applied (electric) field. Together with temperature and an applied pressure, determining whether the lubricant is in a fluidlike isotropic state or in a layered in-plane nematic state, such ordering is found to control the frictional properties of the lubricant. Our extensive molecular dynamics simulations reveal in a detailed manner how friction can be controlled via applied fields. The results are expected to help in designing novel strategies to develop lubricants with dynamically controllable properties.

DOI: 10.1103/PhysRevE.91.012504 PACS number(s): 61.30.Gd, 81.40.Pq

I. INTRODUCTION

Controlling tribological interactions, including friction, wear, and adhesion, is a topic of considerable importance from the point of view of various applications. In particular, without proper control of such effects in micro- and nanoscale mechanical devices, their lifetimes and reliability are severely limited. This has triggered an extensive search for strategies to control friction, ranging from electric field control of polyelectrolyte coatings [1] or ionic liquids [2,3] to applying vibrating normal forces [4,5] to tuning of van der Waals forces [6] and using magnetic nanofluids [7].

Lubricants are often used to reduce the detrimental effects of friction and wear [8]. A particular class of lubricants we focus on in the present study is given by nematic liquid crystals (LCs), which have recently been demonstrated to give rise to low friction coefficients and wear rates [9–14]. LC systems can be characterized by the presence or absence of positional and/or orientational order of the elongated molecules, which is controllable by, e.g., tuning temperature or applying external electric or magnetic fields [15]. In the context of LC lubricants, also applied pressure and sliding velocity of the confining surfaces are expected to play a role [16–20]. On the other hand, lubrication properties of LCs should depend on their ordering [21–23]. Thus, LCs provide a promising system to develop lubricants with controllable properties by applying external fields [24].

To elucidate the fundamental mechanisms via which order and orientation of a nematic lubricant affect its frictional properties, we perform extensive molecular dynamics (MD) simulations of a rigid bead-necklace model of elongated molecules, confined by two rigid, parallel plates in relative sliding motion [21]. Using such a simplified model makes it possible to perform systematic scans of the parameter space, allowing one to gain insight into optimal ways of tuning friction as well as into the underlying physical ordering processes. The equilibrium system displays fluidlike isotropic and layered in-plane nematic phases depending on temperature and the confining pressure [25]. Sliding slowly the top surface gives rise to a preferred in-plane molecular orientation along the sliding direction and leads to a small perturbation of the equilibrium phase diagram. The two phases are found to be correlated with the frictional properties of the lubricant, with higher friction coefficients observed in the fluidlike isotropic phase. Our detailed study of the effect of applied fields reveals that the related tunability of friction is intimately connected to the phase behavior of the lubricant: the largest relative *increase* in friction is obtained when in-plane fields perpendicular to the sliding direction are applied with the system close to the nematic-isotropic transition boundary. Moreover, the largest relative friction *reduction* occurs in the isotropic phase with applied fields along the sliding direction. This article is organized as follows. Section II contains details of the simplified MD simulation model, and the simulation results are presented in Sec. III. Section IV finishes the article with discussions and conclusions.

II. MODEL

The model we study is an extension of a rigid bead-necklace model previously used to simulate the phase behavior of LC systems [26–28] and recently adopted to study stick-slip dynamics in the boundary lubrication (monolayer) regime [21]. Here we investigate the frictional properties of a relatively thick lubricant layer, where $N = 537$ elongated molecules are confined by two parallel plates, with the top one sliding at a constant velocity v (see Fig. 1). The MD simulations are performed with LAMMPS [29]. Each bead-necklace molecule consists of 9 beads, rigidly attached to each other to form a linear, elongated molecule. The two confining rigid surfaces of area A both consist of 2500 beads (identical to the ones of the molecules), arranged in the fcc (100) crystalline structure. Each bead in the system interacts with the others via a Lennard-Jones (LJ) potential, $V_{\mathrm{LJ}}(r) = 4\epsilon[(\sigma/r)^{12} - (\sigma/r)^{6}]$, with ϵ being the depth of the potential well, σ the interaction range, and r the distance between the beads. A Langevin thermostat is used, incorporating the effect of a finite temperature T. Thus, the force acting on bead i of mass m belonging to the molecule S ($i \in S$) is given by

$$m\frac{d^2\mathbf{r}_i}{dt^2} = -\sum_{j\notin S}\frac{d}{d\mathbf{r}_i}V_{\mathrm{LJ}}(|\mathbf{r}_i-\mathbf{r}_j|) - [m\eta v_{i,y}(t)+f_{\mathrm{ran}}]\hat{\mathbf{y}}, \quad (1)$$

where $[\cdots]\hat{\mathbf{y}}$ indicates that the Langevin thermostat acts in the y direction only, to avoid streaming bias. We have checked that applying the Langevin thermostat along z does not change

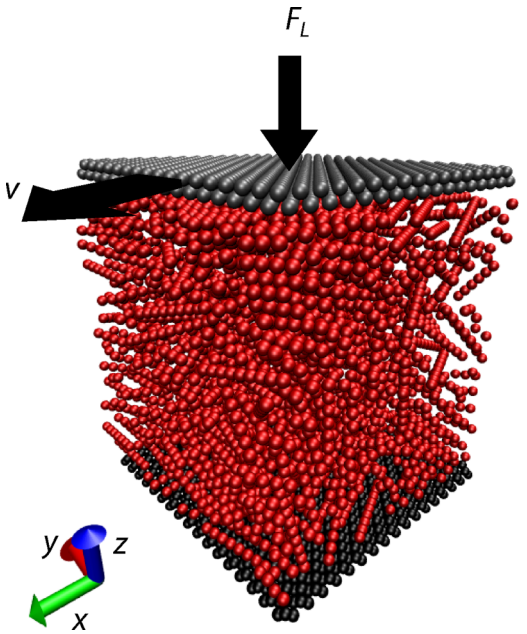

FIG. 1. (Color online) A snapshot of the system in the isotropic phase. The elongated molecules are confined by two parallel plates, with the top one sliding at a constant speed v in the x direction, and subject to a constant normal force, F_L.

the results. $f_{\rm ran}(t)$ satisfies $\langle f_{\rm ran}(t)\rangle = 0$ and $\langle f_{\rm ran}(t) f_{\rm ran}(t')\rangle = 2m\eta k_{\rm B}T\delta(t-t')$. The constraints due to the rigidity of the molecules are taken into account using the *rigid/nve* style implemented in LAMMPS [29,30].

While the bottom plate is fixed at $z = 0$, the top plate is subject to a constant normal force F_L in the $-z$ direction, controlling the pressure $P = F_L/A$ of the lubricant. The equation of motion of the top plate in the vertical z direction is given by

$$M\frac{d^2 Z_{\rm top}}{dt^2} = -\sum_{i\in{\rm top}}\sum_{j\notin{\rm top}}\frac{d}{dz_i}V_{\rm LJ}(|\mathbf{r}_i - \mathbf{r}_j|) - F_L, \qquad (2)$$

where $M = \sum_{i\in{\rm top}} m$ is the mass and $Z_{\rm top} = \frac{1}{N_{\rm top}}\sum_{i\in{\rm top}} z_i$ is the z coordinate of the center of mass of the top plate. We use nondimensional units (LJ units in LAMMPS jargon [29]): $x^* = x/\sigma$, $T^* = Tk_B/\epsilon$, and $t^* = t\sqrt{\epsilon/m\sigma^2}$. In these units, the bead spacing within the LC molecules is 0.6, while the lattice constant of the confining surfaces is 0.5: thus, their ratio is a rational number, and the surface-molecule system is partially commensurate. The time step of the velocity Verlet integrator is set to $\delta t = 0.005$, and η to 0.001. The simulations are initiated by setting the two parallel plates a large distance apart and putting the molecules in between them in a regular initial arrangement with their long axes along x [31]. The plates are then slowly brought closer together, with the molecules finding a more random arrangement due to thermal fluctuations. Finally, after reaching an equilibrium separation between the plates such that the applied normal load is balanced by the internal pressure P, we start to slide the top plate in the x direction with a constant velocity v, in the presence or absence of an external (electric) field $\mathbf{E}$. Ordinary nematics tend to orient along applied electric fields due to the anisotropic dielectric susceptibility of the nematic phase [15]. For simplicity, we model this effect by applying a constant force of magnitude E in the direction of the field to the two outmost beads of every molecule [28]. For each set of parameters (T, P, $\mathbf{E}$) we simulate the system for 25 000 time units ($5\times10^6\delta t$) after reaching the steady state, to compute the steady-state time-averaged friction coefficient $\mu = -\langle F_x(t)\rangle/F_{\rm L}$, where $F_x(t)$ is the x component of the instantaneous force exerted by the lubricant on the top plate.

III. RESULTS

A. Equilibrium phase behavior

The main panel of Fig. 2 shows $Z_{\rm top}$ after equilibration as a function of T and P, for $v, |\mathbf{E}| = 0$. In addition, to characterize the phase behavior of the system, we study both positional and orientational order exhibited by the confined lubricant layer. An example of the T dependence (for a fixed P) of the average absolute values of the components $c_{i,0}$ (with $i \in \{x,y,z\}$; 0 refers to the absence of applied fields) of the unit vector along the long axis of the molecules is shown in the top inset of Fig. 2. In particular, $c_{z,0}$ is found to increase abruptly as T is raised above a "critical" value (here, close to 6.5). This increase corresponds to a change from a low $Z_{\rm top}$ layered configuration (see the density profile along the z direction

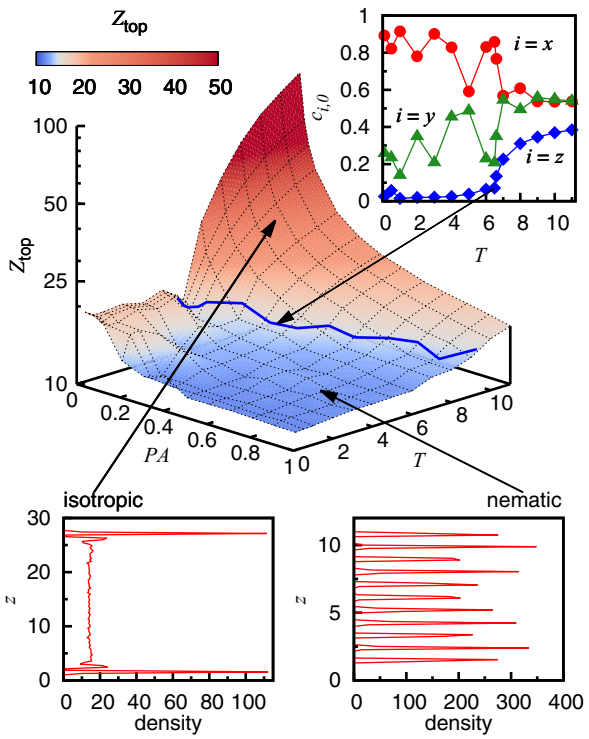

FIG. 2. (Color online) Phase diagram for a system at equilibrium ($v, \mathbf{E} = 0$), showing the equilibrium height $Z_{\rm top}$ of the system as a function of T and P. The solid line separating the two phases (fluidlike isotropic and layered nematic, with typical density profiles shown in the bottom insets) is obtained using as an order parameter the value of the average absolute z-component $c_{z,0}$ of the molecular unit vector (top inset).

in the bottom right inset of Fig. 2) with the long axes of the molecules within the planes of the layers ($c_{z,0} = 0$) to a close to isotropic phase with larger Z_{top} and $c_{z,0} > 0$ where the molecules asymptotically have no preferred orientation. However, as is evident from the behavior of $c_{z,0}$, the confining surfaces have a non-negligible effect for any finite T (and P), and thus the system becomes truly isotropic only in the $T \to \infty$ (or $P \to 0$) limit. No layering is observed in the isotropic phase, except very close to the confining surfaces (see the bottom left inset of Fig. 2). Thus, we use $c_{z,0}$ as an "order parameter" to find a phase boundary (blue line in Fig. 2) separating a low-volume layered nematic phase for low T and/or high P from a close to isotropic phase for high T and/or low P.

The layered low T and/or high P phase thus exhibits a combination of positional and orientational order, with a preferred molecular orientation along x due to the structure of the confining surfaces [21] (a possible small contribution may also originate from the initial configuration). We refer to this state as a layered (in-plane) nematic phase, given that within each confinement-induced layer the molecules exhibit nematic order. Notice that this order is different from typical bulk *smectic* order where the molecules within each layer are either aligned along the layer normal (smectic A) or are tilted with respect to it (smectic C). Also, in the absence of the confining surfaces, our system would exhibit a bulk nematic phase for low temperatures [27,28]. Notice also that the in-plane layered phase includes also a region for low P and T, with a larger Z_{top} than in the rest of the nematic (in-plane) phase (Fig. 2). There the molecules still remain layered, with the increase in height of the system originating from an increase in the spacing between the in-plane molecular layers.

B. Sliding friction without applied fields

After equilibration, we start sliding the top surface with a small velocity $v = 0.5$ (other small v values yield similar results) along the x direction, with $\mathbf{E} = 0$. This results in a small perturbation of the equilibrium phase diagram, Fig. 2, with the $v = 0.5$ phase boundary (black line in the top left panel of Fig. 3; the other three panels are discussed later) almost the same as for $v = 0$, indicating that we are indeed considering the small sliding velocity regime such that the rate of injecting energy into the system due to sliding is low enough not to cause significant changes for the observed phase behavior. The largest μ values are found in the high-volume part (low T and P) of the in-plane nematic phase, while the lowest μ values occur mainly in other parts of the same phase. The isotropic phase exhibits intermediate μ values: while in that case the molecules are largely free to move and dissipate the energy of the moving top plate, the low density of the lubricant implies a relatively weak interaction with the plates, and thus not very high values of μ are observed. In the low-P, high-T isotropic phase, the lubricant exhibits a roughly linear velocity profile across the gap, without visible shear bands. In the more densely packed solidlike layered nematic phase, slip is localized at the lubricant-plate interface (i.e., only wall slip is observed), either at those of both the top and bottom plates or at just one of them (bottom or top, depending on the realization); see Fig. 4 for an example of velocity profiles.

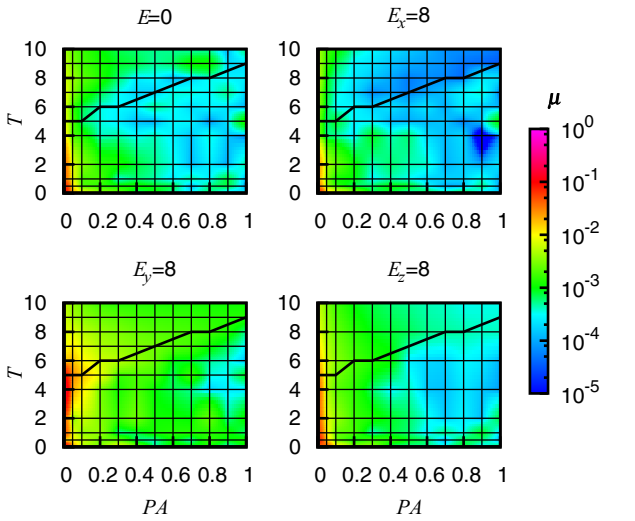

FIG. 3. (Color online) Friction coefficient μ without (top left panel) and with an applied field of magnitude $|\mathbf{E}| = 8$, along x, y, and z in the top right, bottom left, and bottom right panels, respectively. The solid line corresponds to the phase boundary separating the nematic and isotropic phases of the system with $v = 0.5$ and $E = 0$.

Also intermediate solidlike states where slip is localized at the lubricant-plate interfaces exhibiting partial or no layering can be observed; see the middle row and the bottom right panel of Fig. 4.

C. Effect of applied field on sliding friction

Next we explore how applying electric fields $\mathbf{E}$ along x, y, and z modifies the above behavior. To do this, we start by considering two example cases, one corresponding to the fluidlike, isotropic phase, while the other shows the typical behavior of the layered in-plane nematic phase (Fig. 5). The effect of the applied field in different directions, E_i with $i \in \{x,y,z\}$, is clearly different in the two phases: While sufficiently large fields along y tend to always lead to the largest increase in friction, E_x and E_z have almost no effect on μ in the layered nematic phase, while in the isotropic phase E_x tends to decrease friction. To gain more insight into the orientation dependence of the frictional properties, we next consider the field magnitude $|\mathbf{E}| = 8$ (a value large enough to have a clear effect, see Fig. 5) in more detail.

The remaining three panels of Fig. 3 show the dependence of μ on T and P, for different orientations of the external field of magnitude $|\mathbf{E}| = 8$. In particular, a clear increase in μ (as compared to the $|\mathbf{E}| = 0$ case, top left panel of Fig. 3) is seen for $E_y = 8$ (bottom left panel of Fig. 3), especially in the small-P region in the vicinity of the phase boundary (black line) of the $\mathbf{E} = 0$ system. A similar but weaker effect can be observed in the case of $E_z = 8$ (bottom right panel of Fig. 3). Applying the field along x (i.e., the sliding direction) tends to decrease friction, especially for P and T corresponding to the isotropic phase of the $\mathbf{E} = 0$ system.

To highlight the changes induced by the applied fields on friction (with the $|\mathbf{E}| = 0$ case already showing significant variation of μ with T and P), we choose to compute the relative change of μ with respect to the one observed for

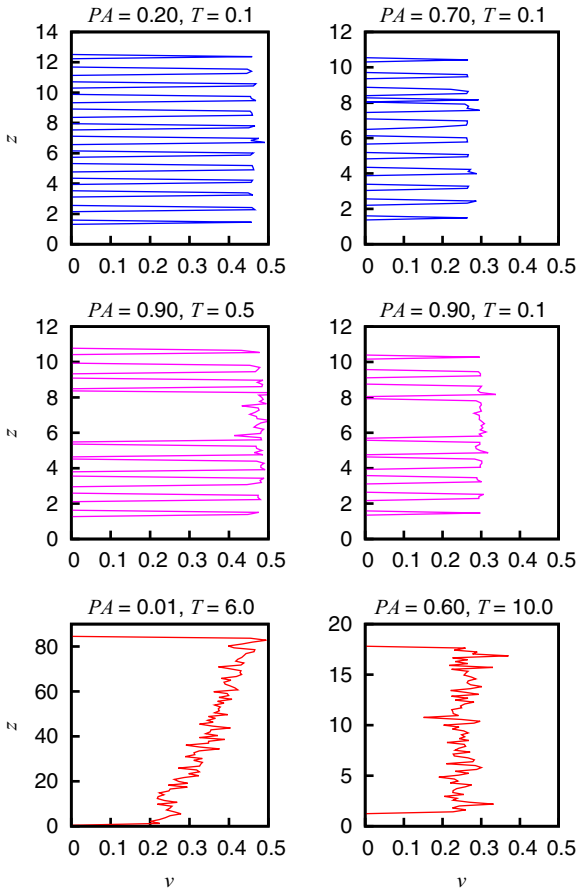

FIG. 4. (Color online) Examples of the velocity profiles of the lubricant for $v = 0.5$ and $E = 0$, for different temperatures and pressures. For high pressures and low temperatures the system tends to exhibit layering (visible as peaks in the velocity profiles), either complete (top row) or partial (middle row). For the layered, solidlike systems, slip is localized at either one (top and middle left panels) or both (top and middle right panels) of the plate-lubricant interfaces. For high temperatures and low pressures the system is no longer layered and may exhibit either a fluidlike linear velocity profile (bottom left panel) or an "amorphous,' nonlayered solidlike behavior. An example where slip takes place at both the top and bottom lubricant-plate interfaces is shown in the bottom right panel.

$|\mathbf{E}| = 0$, $(\mu_E - \mu_0)/\mu_0$, with μ_E and μ_0 being the friction coefficients with and without an applied field, respectively. These are reported for $E_x = 8$, $E_y = 8$, and $E_z = 8$ in the left, middle, and right panels, respectively, in the top row of Fig. 6. There, the largest relative increase in friction is observed close to the nematic-isotropic phase boundary when applying the field in the y direction. A significant increase in friction, again in the proximity of the phase boundary, can also be observed for fields along z. Only a weak dependence on the field along x (i.e., the sliding direction) is observed, with the most notable feature being a decrease of μ in the isotropic, fluidlike phase: There the applied field and the sliding top plate both contribute to order along x, thus reducing the freedom of the molecules to dissipate the energy of the moving top plate.

These observations can be related to changes in the orientation of the LC molecules induced by the applied fields. To quantify this effect, we consider the relative change of

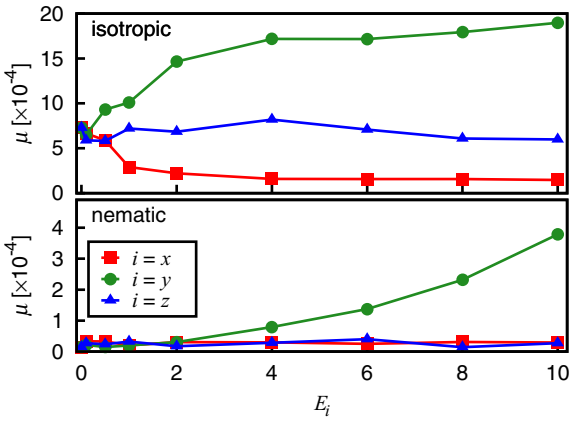

FIG. 5. (Color online) Friction coefficient μ as a function of the external field magnitude E_i, with $i \in x,y,z$. Top: A typical example with the system in the isotropic phase ($P = 0.4$, $T = 9.0$). Bottom: A typical example with the system in the layered nematic phase ($P = 0.7$, $T = 4.0$)

the average orientation of the molecules, $(c_{i,E} - c_{i,0})/c_{i,0}$, where E refers to the applied field and $i \in \{x,y,z\}$. These are reported in the bottom 3×3 grid of Fig. 6. Applying the field in the x direction (first column of Fig. 6) results in the molecules orienting increasingly along x in the isotropic phase (as evidenced by a relative increase of $c_{x,E}$ and a decrease of $c_{y,E}$ and $c_{z,E}$; this behavior coincides with a friction reduction in the isotropic phase). When the field is applied along y or z, the orientation of the molecules changes accordingly mostly in the vicinity of the nematic-isotropic phase boundary. In both cases we observe a clear correlation between the change of orientation of the molecules and an increase of friction. However, the largest relative friction increase is observed for fields along y, while z fields result in the largest relative orientation change of the molecules.

Finally, we discuss qualitatively the physical origins of the changes of the friction coefficient when applying external fields in different directions. First, one should note that the sliding motion of the top plate along x induces a preferred molecular orientation along x. Then, it is natural that if one suppresses any competing effects (due to, e.g., thermal fluctuations) which may induce deviations from this preferred direction, by applying fields parallel to the sliding direction (x direction), the system has effectively less degrees of freedom to dissipate energy. Thus, depending on the phase of the system in the absence of applied fields, applying fields along x may either reduce friction (isotropic phase, where thermal effects are important), or keep it constant (layered nematic phase). The latter effect arises since the system without applied fields already has the molecules along x in a close to solidlike arrangement, and thus the application of the field along x does not change the molecular orientation, leaving also friction unaffected. In contrast to this behavior, applying the field along y (perpendicular to the sliding direction, but in-plane) results in a competition between the field and sliding-induced orientation mechanisms. Consequently, the resulting molecular orientation along y is not as stable as the one in the case of fields along x, and thus the lubricant is more susceptible to perturbations induced by the interaction

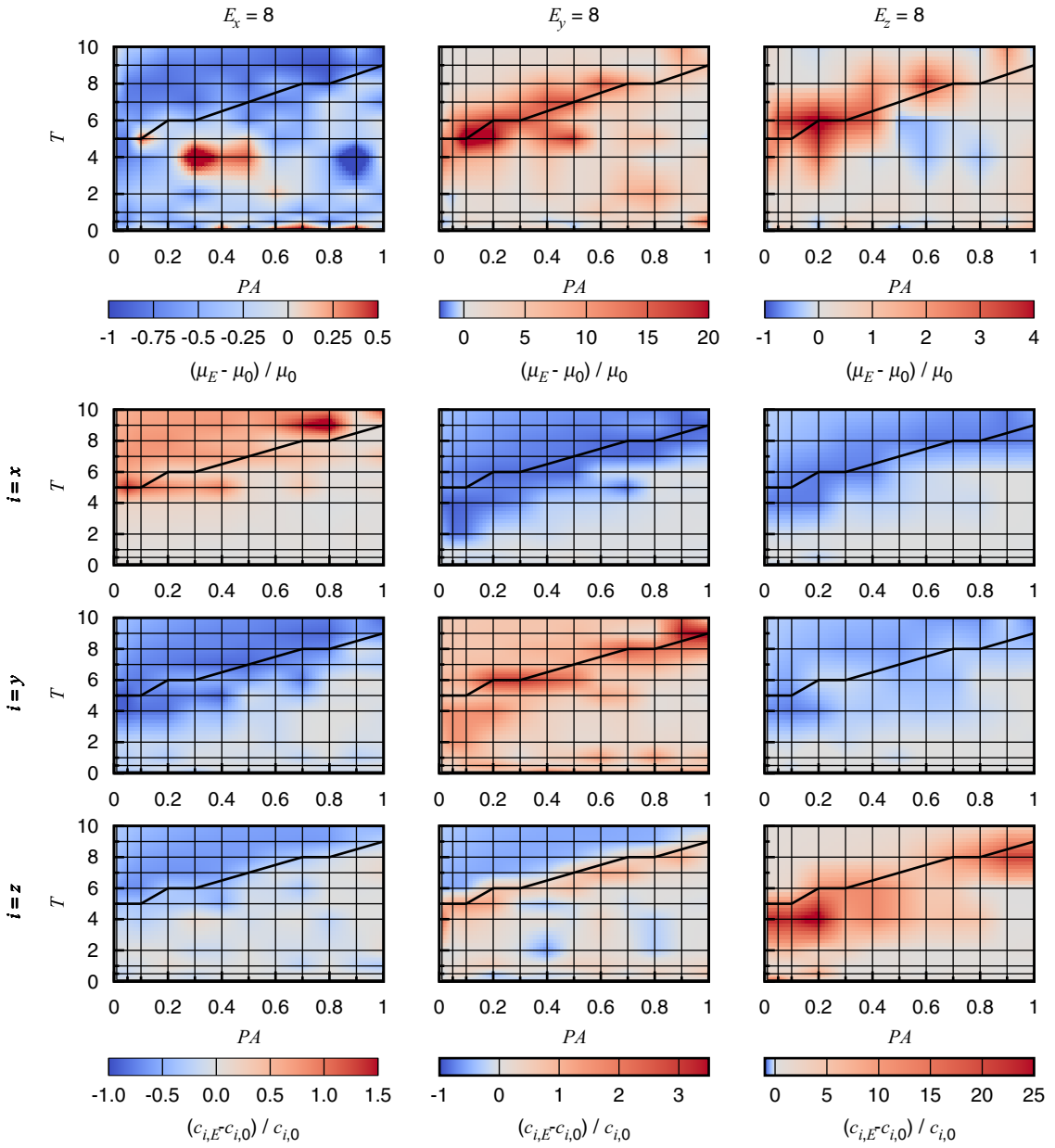

FIG. 6. (Color online) Top row: Relative change of the friction coefficient, $(\mu_E - \mu_0)/\mu_0$, as compared to the no-field case, for a field of magnitude $|\mathbf{E}| = 8$ in the x, y, and z directions. Bottom rows: The corresponding relative changes in the average direction of the molecules $(c_{i,E} - c_{i,0})/c_{i,0}$, with $i = x$, y, and z shown in the top, middle, and bottom rows, respectively. Notice the different scales in the color bars corresponding to different field directions.

with the confining surfaces. This implies that the molecules are also more susceptible to dissipating energy, and thus the friction force is higher. Finally, fields along z do lead to a moderate increase in friction close to the nematic-isotropic phase boundary. Again, this increase should relate to the z orientation of the molecules not being a stable state (as the competing effect due to sliding is also operating), and consequently the resulting molecular motion dissipates energy. One should notice that when the molecules exhibit a nonzero orientation along z, the volume of the system increases, and thus the density of the lubricant goes down. This implies that the net interaction between the lubricant and the confining surfaces is weaker as compared to the more dense systems with in-plane molecular orientation. Thus, while friction increases due to the molecular orientation not being a stable state, the effect is weaker than that for fields along y since the overall surface-lubricant interaction is weaker due to the lower density of the lubricant.

IV. CONCLUSIONS

To conclude, we have presented a phase diagram of a confined LC system under shear and have shown that μ depends on the ordering of the lubricant. This is in qualitative agreement with experiments on systems such as 8CB LCs confined by mica surfaces, displaying, e.g., an anisotropic critical shear stress [23]. Thus, a possibility to control friction by tuning the LC orientation by external fields emerges. The

largest relative friction increase is obtained when applying in-plane fields perpendicular to the sliding direction close to the nematic-isotropic transition boundary, while the largest relative reduction of μ occurs in the isotropic phase with applied fields along the sliding direction. These findings may open up interesting possibilities to dynamically tune the frictional properties of LC lubricants by applying external fields.

Some final remarks are in order. Due to numerical limitations, our study has been constrained to one system size. Lubricated friction may involve size effects, manifested, e.g., as the various lubrication regimes such as boundary, mixed, and hydrodynamic lubrication. Thus, while our lubricant layer is certainly thick enough such that we are not close to the monolayer boundary-lubricated regime where, e.g., stick-slip dynamics may ensue [21], we might still expect some dependence of μ on the system size. Also the details of the LC-surface interaction, which we here have for simplicity assumed to be the same as those of the LC-LC one, and the commensurate and/or incommensurate nature of the molecular structure and that of the confining surfaces should play a role when it comes to the precise value of μ. However, our focus here has been on understanding the *relative change* of μ when external fields are applied, affecting the orientation of the elongated molecules of the lubricant. It would be interesting to extend the study to MD simulations of full atomistic models of LC molecules (5CB, 6CB, 8CB, etc.), confined by atomistic surfaces. In that context, also the role of surface anchoring (possibly leading to a molecular alignment perpendicular to the confining surfaces [9]), various lubricant additives in addition to the LCs, etc., could be addressed. Additional experimental checks of the tunability of friction in LC systems by external fields should also be performed [24].

ACKNOWLEDGMENTS

We acknowledge the financial support of the Academy of Finland through an Academy Research Fellowship (L.L., Project No. 268302) and via the Centres of Excellence Program (Project No. 251748). The numerical simulations presented above were performed using computer resources within the Aalto University School of Science "Science-IT" project.

[1] C. Drummond, Phys. Rev. Lett. **109**, 154302 (2012).
[2] J. Sweeney, F. Hausen, R. Hayes, G. B. Webber, F. Endres, M. W. Rutland, R. Bennewitz, and R. Atkin, Phys. Rev. Lett. **109**, 155502 (2012).
[3] S. Perkin, Phys. Chem. Chem. Phys. **14**, 5052 (2012).
[4] R. W. Carpick, Science **313**, 184 (2006).
[5] A. Socoliuc *et al.*, Science **313**, 207 (2006).
[6] M. Lessel, P. Loskill, F. Hausen, N. N. Gosvami, R. Bennewitz, and K. Jacobs, Phys. Rev. Lett. **111**, 035502 (2013).
[7] E. Andablo-Reyes, R. Hidalgo-Alvarez, and J. de Vicente, Soft Matter **7**, 880 (2011).
[8] B. J. Hamrock, S. R. Schmid, and B. O. Jacobson, *Fundamentals of Fluid Film Lubrication* (CRC Press, Boca Raton, FL, 2004).
[9] C. Tadokoro, T. Nihira, and K. Nakano, Tribol. Lett. **56**, 239 (2014).
[10] R. J. Bushby and K. Kawata, Liq. Cryst. **38**, 1415 (2011).
[11] T. Amann and A. Kailer, Wear **271**, 1701 (2011).
[12] T. Amann and A. Kailer, Tribol. Lett. **41**, 121 (2011).
[13] F.-J. Carrion, G. Martinez-Nicolas, P. Iglesias, J. Sanes, and M.-D. Bermudez, Int. J. Mol. Sci. **10**, 4102 (2009).
[14] A. Kailer, T. Amann, G. Konrath, D. Janietz, and H. Sawade, in *Friction, Wear and Wear Protection*, edited by A. Fisher and K. Bobzin (Wiley-VCH Verlag GmbH & Co, Weinheim, Germany, 2009).
[15] P. G. de Gennes and J. Prost, *The Physics of Liquid Crystals* (Oxford University Press, London, 1995).
[16] L. Noirez, G. Pepy, and P. Baroni, J. Phys.: Condens. Matter **17**, S3155 (2005).
[17] C. Pujolle-Robic and L. Noirez, Phys. Rev. E **68**, 061706 (2003).
[18] S. H. J. Idziak, C. R. Safinya, R. S. Hill, K. E. Kraiser, M. Ruths, E. Warriner, S. Steinberg, K. S. Liang, and J. N. Israelachvili, Science **264**, 1915 (1994).
[19] M. Ruths, S. Steinberg, and J. N. Israelachvili, Langmuir **12**, 6637 (1996).
[20] J. Janik, R. Tadmor, and J. Klein, Langmuir **13**, 4466 (1997).
[21] W. Chen, S. Kulju, A. S. Foster, M. J. Alava, and L. Laurson, Phys. Rev. E **90**, 012404 (2014).
[22] C. Cheng, L. Kellogg, S. Shkoller, and D. Turcotte, Proc. Natl. Acad. Sci. U.S.A. **105**, 7930 (2008).
[23] A. Artsyukhovich, L. D. Broekman, and M. Salmeron, Langmuir **15**, 2217 (1999).
[24] Y. Kimura, K. Nakano, and T. Kato, Wear **175**, 143 (1994).
[25] J. Klein and E. Kumacheva, J. Chem. Phys. **108**, 6996 (1998).
[26] P. Tian, D. Bedrov, G. D. Smith, M. Glaser, and J. E. Maclennan, J. Chem. Phys. **117**, 9452 (2002).
[27] P. Tian and G. D. Smith, J. Chem. Phys. **116**, 9957 (2002).
[28] P. Tian, D. Bedrov, G. D. Smith, and M. Glaser, J. Chem. Phys. **115**, 9055 (2001).
[29] S. J. Plimpton, J. Comp. Phys. **117**, 1 (1995); http://lammps.sandia.gov.
[30] T. F. Miller III *et al.*, J. Chem. Phys. **116**, 8649 (2002).
[31] This choice of the initial molecular orientation decreases the transient time before reaching the steady state after sliding of the top plate in the x direction is initiated.